S100A1: A regulator of myocardial contractility

Patrick Most*, Juliane Bernotat*, Philipp Ehlermann*, Sven T. Pleger*, Michael Reppel*, Melanie Börries*, Ferraydoon Niroomand†, Burkert Pieske‡, Paul M. L. Janssen‡§, Thomas Eschenhagen¶, Peter Karczewski‖, Godfrey L. Smith, Walter J. Koch††, Hugo A. Katus*, and Andrew Remppis*‡‡**

*Medizinische Klinik II, Medizinische Universität zu Lübeck, 23538 Lübeck, Germany; †Abteilung Innere Medizin III, Medizinische Universität Heidelberg, 69115 Heidelberg, Germany; ‡Abteilung Kardiologie und Pneumologie, Zentrum Innere Medizin, Universität Göttingen, 37075 Göttingen, Germany; §Johns Hopkins School of Medicine, Division of Cardiology, Baltimore, MD 21205; ¶Institut für Experimentelle und Klinische Pharmakologie und Toxikologie, Universität Erlangen, 91054 Erlangen, Germany; ‖Max Delbrück Zentrum, Berlin-Buch, 13125 Berlin, Germany; **Institute of Biomedical Life Science, University of Glasgow, G128QQ Glasgow, Scotland; and ††Department of Surgery, Duke University Medical Center, Durham, NC 27710

Edited by Eugene Braunwald, Partners HealthCare System, Inc., Boston, MA, and approved September 24, 2001 (received for review July 27, 2001)

S100A1, a Ca^{2+} binding protein of the EF-hand type, is preferentially expressed in myocardial tissue and has been found to colocalize with the sarcoplasmic reticulum (SR) and the contractile filaments in cardiac tissue. Because S100A1 is known to modulate SR Ca^{2+} handling in skeletal muscle, we sought to investigate the specific role of S100A1 in the regulation of myocardial contractility. To address this issue, we investigated contractile properties of adult cardiomyocytes as well as of engineered heart tissue after S100A1 adenoviral gene transfer. S100A1 gene transfer resulted in a significant increase of unloaded shortening and isometric contraction in isolated cardiomyocytes and engineered heart tissues, respectively. Analysis of intracellular Ca^{2+} cycling in S100A1-overexpressing cardiomyocytes revealed a significant increase in cytosolic Ca^{2+} transients, whereas in functional studies on saponin-permeabilized adult cardiomyocytes, the addition of S100A1 protein significantly enhanced SR Ca^{2+} uptake. Moreover, in Triton-skinned ventricular trabeculae, S100A1 protein significantly decreased myofibrillar Ca^{2+} sensitivity ([$EC_{50\%}$]) and Ca^{2+} cooperativity, whereas maximal isometric force remained unchanged. Our data suggest that S100A1 effects are cAMP independent because cellular cAMP levels and protein kinase A-dependent phosphorylation of phospholamban were not altered, and carbachol failed to suppress S100A1 actions. These results show that S100A1 overexpression enhances cardiac contractile performance and establish the concept of S100A1 as a regulator of myocardial contractility. S100A1 thus improves cardiac contractile performance both by regulating SR Ca^{2+} handling and myofibrillar Ca^{2+} responsiveness.

The protein S100A1 is a Ca^{2+} binding protein of the EF-hand type and a member of the S100 protein family. To date, 19 different genes for this protein family have been identified, all exhibiting a unique spatial and temporal expression pattern (1). S100 proteins have been reported to be involved in different biological activities such as transduction of intracellular Ca^{2+} signaling and cytoskeleton-mediated interactions as well as cell-cycle progression, cell differentiation, and other functions (2). S100A1 is especially interesting with respect to muscle physiology as it is the most abundant S100 protein in striated muscle and preferentially expressed in myocardial tissue (3). Interestingly, this protein has been found to colocalize with the sarcoplasmic reticulum (SR) and the contractile filaments in cardiac tissue (4). Moreover, recent studies of our own group revealed a differential expression of S100A1 with diminished protein levels in cardiomyopathy, whereas in compensated hypertrophy S100A1 protein was found to be up-regulated (5, 6). Thus, alterations in the expression of this protein might very well contribute to impaired sarcoplasmic Ca^{2+} handling in end-stage heart failure, a fact that was first described by the group of Schwartz *et al.* (7). These data prompted us to hypothesize that S100A1 might be involved in the regulation of cardiac contractility. Therefore in the current study, we investigated the impact of enhanced S100A1 expression on contractile performance, intracellular Ca^{2+} cycling, sarcoplasmic Ca^{2+} uptake, sarcomeric Ca^{2+} sensitivity, and cAMP homeostasis in various cardiomyocyte and myocardial tissue preparations.

Methods

S100A1 Purification of Native Protein. Native S100A1 protein was purified from porcine left ventricular myocardium as previously described (8).

Generation of S100A1 Adenovirus. The construction, production, and purification of adenoviral constructs containing either green fluorescent protein (GFP) alone (AdvGFP) or GFP with human S100A1 cDNA (AdvS100A1, accession number X58079) were carried out with a first-generation E1/E3 deleted, replication-deficient adenovirus as previously published (9). Both transgenes were under the control of a cytomegalovirus promoter.

Isolation and Transfection of Adult Ventricular Rabbit Cardiomyocytes. Ca^{2+} tolerant adult cardiomyocytes were isolated from left ventricular tissue of rabbits by a standard enzymatic digestion procedure and cultivated as described (10). Adenoviral infection (AdvS100A1, AdvGFP) was performed with a multiplicity of infection of 20 plaque-forming units/cell 2 h after isolation.

Myocyte Contractile Parameters. The video edge detection of cultured adult rabbit cardiomyocytes was performed as described (11) 24 h after adenoviral-mediated gene transfer. Five consecutive steady-state twitches for each myocyte (AdvS100A1, AdvGFP, and wild type) at 1 Hz, 37°C and 1.8. mM $[Ca^{2+}]_e$ were averaged and analyzed online (LABVIEW 4.01, National Instruments, Austin, TX).

S100A1, SERCA2a/PLB, Calsequestrin (CSQ) Protein, and Phospholamban (PLB) Phosphorylation Levels. Western blotting for S100A1, sarcoplasmic reticulum Ca^{2+} ATPase (SERCA2a), PLB, CSQ, and PLB phosphorylation level (Ser-16/Thr-17) from AdvS100A1, AdvGFP, and wild-type (WT) cardiomyocytes was carried out as previously described (12, 13). Custom-made anti-S100A1 polyclonal affinity-purified antibody was raised in rabbit against the human S100A1 hinge region peptide (amino acid 42–54) that crossreacts with human and rabbit S100A1 protein (Eurogentec, Brussels). Anti-SERCA2a (sc-8095) was purchased from Santa Cruz Biotechnology. Anti-PLB (MA3–922) was from Affinity Bioreagents (Neshanic Station, NJ), and

This paper was submitted directly (Track II) to the PNAS office.

Abbreviations: SR, sarcoplasmic reticulum; EHT, engineered heart tissue; GFP, green fluorescent protein; WT, wild type; PLB, phospholamban; CSQ, calsequestrin; SERCA, sarcoplasmic reticulum Ca^{2+} ATPase.

‡‡To whom reprint requests should be addressed. E-mail: remppis@medinf.mu-luebeck.de.

The publication costs of this article were defrayed in part by page charge payment. This article must therefore be hereby marked "*advertisement*" in accordance with 18 U.S.C. §1734 solely to indicate this fact.

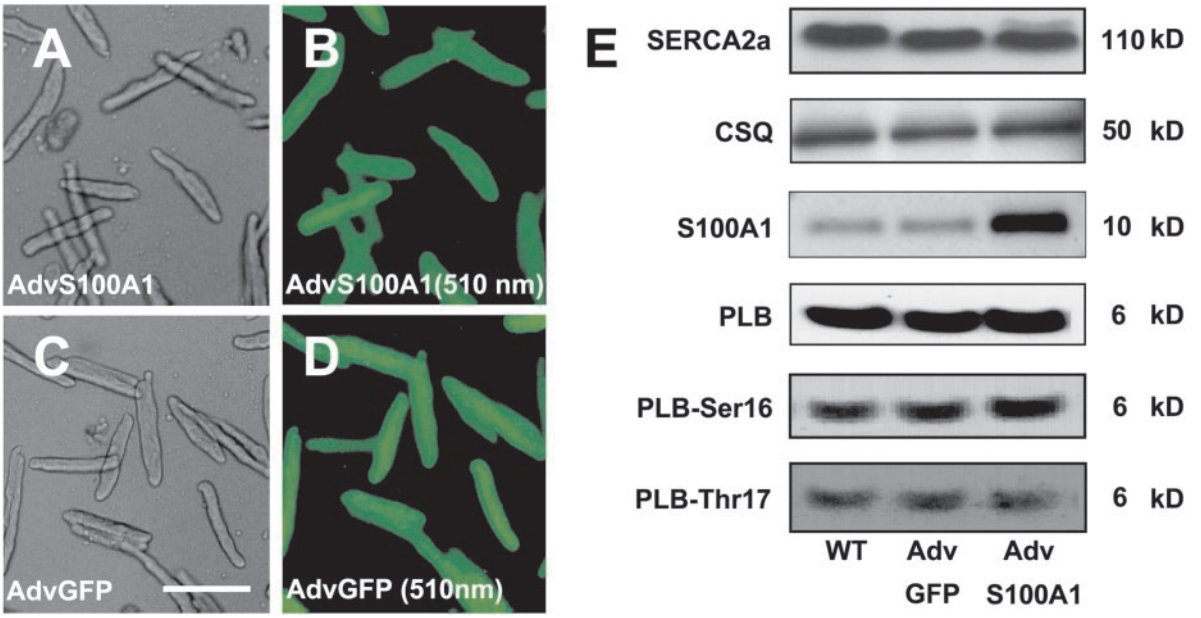

Fig. 1. Efficiency of adenoviral-mediated gene transfer into primary cardiomyocytes. Representative transmission and GFP emission images from adult rabbit ventricular cardiomyocytes 24 h following adenoviral infection. (*A*) AdvS100A1 transmission, (*B*) AdvS100A1 510-nm emission, (*C*) AdvGFP transmission, and (*D*) AdvGFP 510-nm emission are shown. (Bar = 100 μm). (*E*) Effect of S100A1 adenoviral-mediated gene transfer on SERCA2a, CSQ, S100A1, PLB protein expression, and PLB-Ser-16/Thr-17 phosphorylation state after 24 h. Representative SDS/PAGE analysis of extracts from WT, GFP control virus (AdvGFP), and S100A1 virus (AdvS100A1) transfected rabbit cardiomyocytes. (*Right*) M_r are indicated as kDa (n = 3).

anti-phospho-PLB-Ser^{16} (PS-16) and anti-phospho PLB-Thr^{17} (PS-17) were from Fluorescence (Glasgow, U.K.). Anti-CSQ was obtained from Swant (Bellinzona, Suisse).

Three-Dimensional Engineered Heart Tissue (EHT). EHT from neonatal rat cardiomyocytes were produced as previously published (14). EHT with a size of 11 × 6 × 0.4 mm (length × width × thickness) were grown in DMEM, adenovirally transfected on day 8 (multiplicity of infection 10 plaque-forming units/cell). On day 14, isometric force was measured throughout a stepwise increase of Ca^{2+} concentrations ranging from 0.4 to 2.4 mM under electrical stimulation at 2 Hz. Data acquisition and analyses were performed with a PC-assisted system (BMON-2, Ingenieurbüro Jäckel, Hanau, Germany).

Ca^{2+} Transient Analyses. Intracellular Ca^{2+} transients of Indo 1-AM loaded rabbit adult cardiomyocytes (AdvS100A1, AdvGFP, WT) after 24 h were analyzed as previously described (15). Data from five consecutive steady-state transients at 1 Hz, 37°C, and 1.8 mM $[Ca^{2+}]_e$ were averaged for each myocyte and analyzed with Labview 4.01.

Sarcoplasmic Ca^{2+} Uptake. Sarcoplasmic Ca^{2+} uptake in β-escin-skinned rabbit ventricular cardiomyocytes was performed as described elsewhere (16). The Ca^{2+} binding constant for S100A1 was taken from Baudier *et al.* (17). S100A1 interventions were done for 1 μM protein, and S100A1 storage buffer served as control.

Ca^{2+} Sensitivity of Contractile Apparatus. Measurements of the pCa-force relationship in Triton-skinned rabbit ventricular trabeculae (average length/width/thickness: 3,500 ± 300/153 ± 30/124 ± 27 μm) were done as described previously (18, 19). S100A1 protein (1 μM) interventions were done at a sarcomeric length adjusted to 2.2 μm set by laser diffraction.

Intracellular cAMP Measurements. Intracellular cAMP was measured 24 h following transfection with a competitive enzyme immunoassay kit as outlined by the manufacturer (cAMP EIA, RPN 225; Amersham Pharmacia). Measurements were performed in quiescent and 1 Hz field-stimulated cardiomyocytes (AdvS100A1, AdvGFP, WT).

Statistical Analyses. Data are expressed as means ± SEM. Statistical analysis was performed by using ANOVA. A value of $P < 0.05$ was accepted as statistically significant.

Results

S100A1 Improves Contractility of Adult Ventricular Cardiomyocytes. To study the functional significance of elevated S100A1 protein levels in adult rabbit ventricular cardiomyocytes, we overexpressed this protein by adenoviral-mediated gene delivery and analyzed myocyte contractility with video edge detection. Fig. 1 (*B* and *D*) illustrates efficiency of adenoviral transfection for AdvS100A1 and AdvGFP, respectively. As expected (20), coexpression of the GFP reporter indicates that S100A1 is expressed in nearly 100% of AdvS100A1-infected cardiomyocytes after 24 h (Fig. 1*B*). Fig. 1*E* depicts representative Western blot analysis carried out for either S100A1 or other SR proteins in Adv-infected or WT cardiomyocytes. Treatment with AdvS100A1, normalized to CSQ, resulted in a 5.4 ± 0.6-fold increase in total S100A1 protein levels compared with either AdvGFP-treated or WT cardiomyocytes ($P < 0.05$). Importantly, there was no alteration in S100A1 levels in AdvGFP-treated myocytes compared with untreated WT cardiomyocytes. Fig. 2*A* shows superimposed representative contractions taken from AdvS100A1 and AdvGFP-infected cardiomyocytes. Fig. 2*B* demonstrates that S100A1 overexpression caused a marked increase of fractional shortening (5.5 ± 1.7%) compared with AdvGFP control cells (3.0 ± 0.8%). Fig. 2 (*C* and *D*) illustrates that this effect was accompanied by a significant acceleration in the rate of myocyte shortening (−dl/dt, AdvS100A1; 13.0 ± 2.7 vs. AdvGFP; 9.1 ± 2.0 μm/s), and relengthening (+dl/dt, AdvS100A1; 15.8 ± 3.0 vs. AdvGFP; 8.8 ± 3.7 μm/s). For all parameters tested, WT cardiomyocytes exhibited no significant

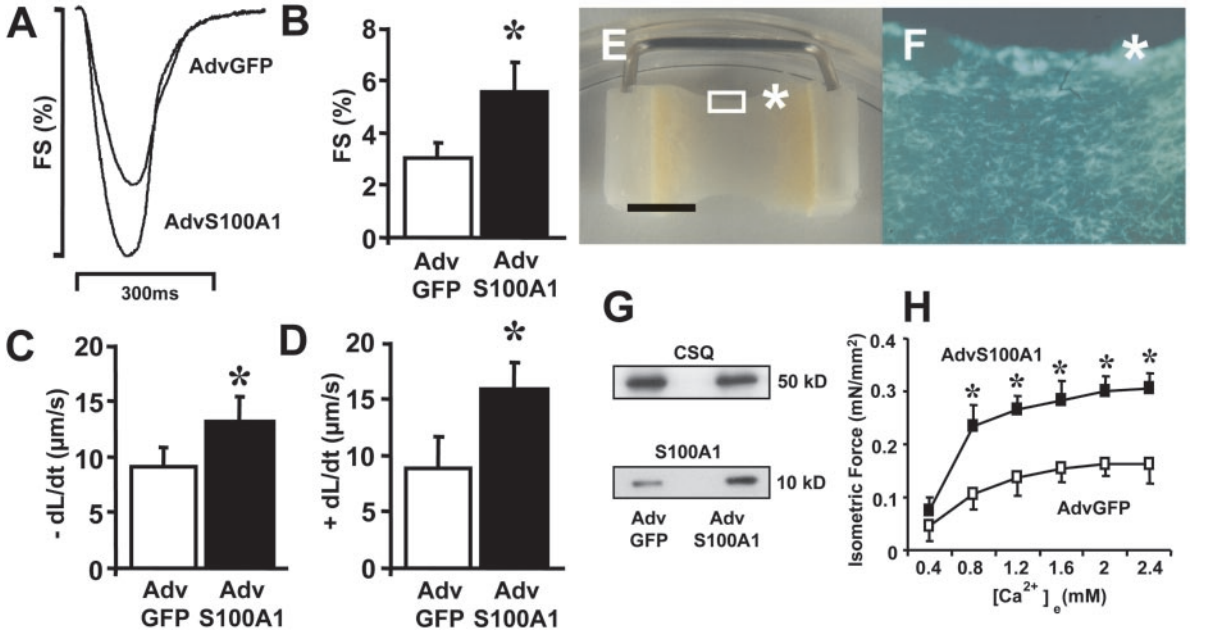

Fig. 2. Effect of S100A1 overexpression on unloaded shortening of adult rabbit ventricular cardiomyocytes and on isometric force of EHT. (*A*) Original superimposed tracings of fractional shortening (FS%; shown as downward deflection) from a representative S100A1 overexpressing (AdvS100A1) and control virus (AdvGFP) infected cardiomyocyte. (*B*) Increase of fractional shortening (FS%), (*C*) rate of myocyte shortening (−dl/dt), and (*D*) rate of myocyte relengthening (+dl/dt) by S100A1 overexpression. Data are mean ± SEM. *, $P < 0.05$ vs. control ($n = 55$). (*E*) A representative S100A1-transfected EHT after a 14-day culture period (original magnification ×5) before measurement. (Bar = 5 mm.) (*F*) *Inset* from *E* (asterisk, original magnification ×40) showing the concaval edge of EHT. GFP coexpression demonstrates S100A1 expression in >95% of the cells. Infection with AdvGFP resulted in similar transfection efficiency (data not shown). (*G*) S100A1 protein overexpression in EHT as confirmed by representative Western Blot analysis of homogenates from control (AdvGFP) and S100A1 (AdvS100A1) transfected EHT. S100A1 protein was normalized to CSQ. (*Right*) M_r are indicated as kDa ($n = 3$). (*H*) Increase of isometric force (mN/mm²) at 2 Hz after S100A1 gene transfer throughout a series of Ca^{2+} activation (0.4–2.4 mM). Data are mean ± SEM. *, $P < 0.05$ vs. control ($n = 10$).

difference compared with AdvGFP-treated cells (data not shown).

S100A1 Increases Isometric Force of Engineered Heart Tissue. To test the impact of S100A1 overexpression on isometric contraction, we produced EHT. EHTs are three-dimensional synthetic cardiac tissues of neonatal cardiomyocytes that retain many physiological characteristics of cardiac tissue and are powerful tools to test transgenes on physiological conditions of isometric contraction (21). EHTs were infected either with AdvS100A1 or AdvGFP on day 8. On day 14 when EHTs were tested, transfection rate approached 100%. Fig. 2*E* demonstrates a typical 14-day-old EHT after infection with S100A1 adenovirus (AdvS100A1) before measurement. Note the concentration of GFP-positive cells at the concaval edge of the EHT (Fig. 2*F*). Western blot analyses revealed a 3.3 ± 0.7-fold increase of total S100A1 protein in AdvS100A1-transfected EHTs compared with AdvGFP-treated EHTs (Fig. 2*G*, $P < 0.05$). Results of isometric measurements are summarized in Fig. 2*H*. In both groups of EHTs (AdvS100A1, AdvGFP), increments in $[Ca^{2+}]_e$ between 0.4 to 2.4 mM evoked an enhanced generation of isometric force. S100A1-overexpressing EHTs, however, responded to increasing $[Ca^{2+}]_e \geq 0.8$ mM with a significantly higher active tension development than AdvGFP-infected EHTs rising isometric force at 2 mM $[Ca^{2+}]_e$ from 0.16 ± 0.02 to 0.30 ± 0.03 mN/mm².

S100A1 Enhances Intracellular Ca^{2+} Transients in Adult Ventricular Cardiomyocytes. Because we were interested in whether the enhancement in contractile performance of S100A1-transfected cellular preparations were related to an increase in cytosolic Ca^{2+} cycling, intracellular Ca^{2+} transients were measured by use of the Indo-1 fluorescence indicator. Fig. 3*A* shows superimposed representative fluorescence ratios comparing S100A1 (AdvS100A1) and control (AdvGFP) infected cardiomyocytes. S100A1 overexpression raised the Ca^{2+} transient amplitude (ratio 405/485 nm) from 0.081 ± 0.019 to 0.137 ± 0.022 compared with control (Fig. 3*B*), whereas time to peak decreased from 159 ± 14 to 120 ± 12 ms, respectively (Fig. 3*C*). Furthermore, S100A1 overexpression also accelerated the decline of cytosolic Ca^{2+} because time to 50% decay shortened from 137 ± 13 to 110 ± 13 ms compared with control. (Fig. 3*D*). Thus, the improvement in cellular contractility seems to be associated with an acceleration in cytosolic Ca^{2+} cycling by S100A1.

Unchanged Expression of SERCA/PLB After S100A1 Overexpression. SR Ca^{2+} cycling depends largely on the SERCA2a/PLB ratio. Thus, we investigated the influence of S100A1 overexpression on SERCA2a and PLB protein levels. Fig. 1*E* illustrates that the expression of these proteins (SERCA2a/PLB) 24 h after AdvS100A1 infection was unchanged.

S100A1 Increases Ca^{2+}-Dependent SR Ca^{2+} Uptake. Because the enhancement of intracellular Ca^{2+} transients by S100A1 did not rely on altered expression of SERCA2a/PLB, we sought to directly measure the impact of S100A1 on SR Ca^{2+} uptake capacity. Accordingly, we chose a model of chemically skinned cardiomyocytes that allows functional investigations of the intact SR. Ca^{2+} uptake into the SR was measured indirectly by monitoring the decay of extra-sarcoplasmic Fura-2 fluorescence after the addition of S100A1 protein. Fig. 3*E* depicts a representative tracing of the decay of extra-sarcoplasmic Ca^{2+} concentration ($[Ca^{2+}]_{es}$), demonstrating a steeper SR Ca^{2+} uptake after the addition of S100A1 protein (1 µM) compared with control. Although the calculated rate of SR Ca^{2+} uptake in cells increased with incremental $[Ca^{2+}]_{es}$ concentrations (0.2–1 µM)

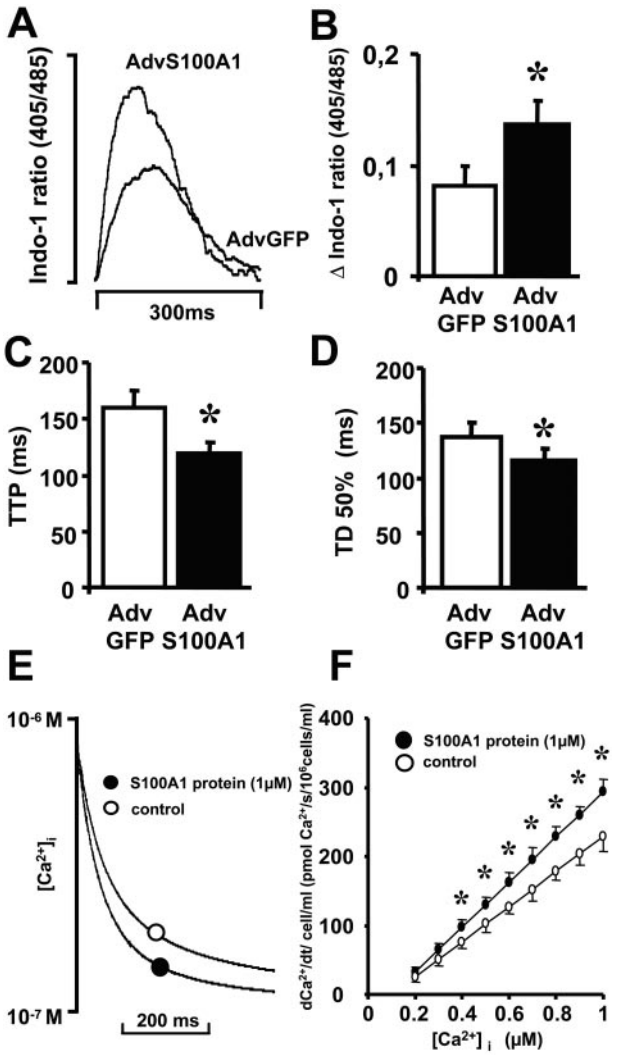

Fig. 3. Effect of S100A1 overexpression on intracellular Ca^{2+} transients of adult rabbit ventricular cardiomyocytes and of S100A1 protein on SR Ca^{2+} uptake. (*A*) Superimposed original tracings of cytosolic Ca^{2+} transients (shown as upward deflection) in a representative S100A1-overexpressing (AdvS100A1) and control-transfected (AdvGFP) cardiomyocyte. (*B–D*) Increase of Ca^{2+} transient amplitude (Δ Indo 1 ratio 405/485 nm) and decrease of time to peak and time to 50% decay of cytosolic Ca^{2+} signal in S100A1-overexpressing cardiomyocytes. Data are mean ± SEM. *, $P < 0.05$ vs. control ($n = 75$). (*E*) Typical original tracings of cytosolic Ca^{2+} decline in β-escin-skinned cardiac myocytes for S100A1 protein (●) and control (○). (*F*) Calculated rate of sarcoplasmic Ca^{2+} uptake (pmol Ca^{2+}/s per 10^6 cells/ml) for S100A1 protein (●) and control (○). Data are mean ± SEM. *, $P < 0.05$ vs. control ($n = 8$).

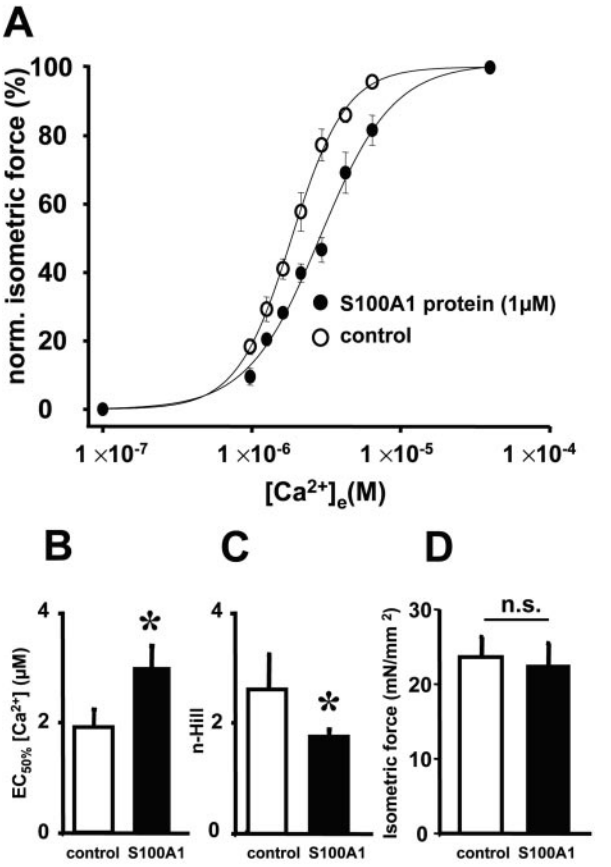

Fig. 4. Effect of S100A1 protein on myofibrillar Ca^{2+} response of rabbit Triton-skinned ventricular trabeculae. (*A*) S100A1-mediated rightward shift of the pCa-force relationship given as Hill regression curve. (*B–D*) Decrease of Ca^{2+} sensitivity ($[EC_{50\%}]$) and Ca^{2+} cooperativity (n-Hill) by S100A1, whereas isometric force (mN/mm^2) was not affected. Data are mean ± SEM. *, $P < 0.05$ vs. control ($n = 7$).

under control conditions, Ca^{2+} uptake rates were significantly higher in cells loaded with S100A1 protein at all $[Ca^{2+}]_{es} \geq 4 \times 10^{-7}$ M (Fig. 3*F*). The addition of 1 μM S100A1 protein resulted in a maximal Ca^{2+} uptake of 293 ± 18 pmol Ca^{2+}/s per 10^6 cells, whereas in controls, Ca^{2+} uptake amounted to 229 ± 21 pmol Ca^{2+}/s per 10^6 cells at 1 μM free $[Ca^{2+}]_{es}$.

S100A1 Decreases Myofilament Ca^{2+} Sensitivity. Because S100A1 has been shown to bind to the contractile apparatus (4) and speed of relaxation also relies on the Ca^{2+} sensitivity of contractile proteins (22), we investigated the influence of S100A1 protein on myofilament Ca^{2+} response (pCa-force relationship). To directly test this, we chose the model of Triton-skinned right ventricular trabeculae from rabbits. Fig. 4*A* demonstrates the influence of S100A1 protein (1 μM) on the pCa-force relationship that results both in a rightward shift of the Hill regression curve and a diminished slope. S100A1 increased the Ca^{2+} concentration for half-maximal force development ($EC_{50\%}$) from 1.9 ± 0.3 μM (control) to 3.0 ± 0.5 μM $[Ca^{2+}]_e$ (Fig. 4*B*) and decreased Ca^{2+} cooperativity (n-Hill) from 2.6 ± 0.6 (control) to 1.8 ± 0.1 (Fig. 4*C*). Fig. 4*D* depicts that S100A1 had no significant effect on maximal force development (22.8 ± 3.0 mN/mm^2) compared with control (23.6 ± 2.6 mN/mm^2).

Effect of S100A1 Gene Transfer on Cellular cAMP Levels and Protein Kinase A Activity. Because S100A1 effects on cell contractility might be explained by increased intracellular cAMP levels, we tested the influence of S100A1 protein overexpression on intracellular cAMP levels. Moreover, we investigated a critical target of cAMP-dependent protein kinase A, PLB phosphorylation. Fig. 5*A* illustrates the influence of S100A1 on cellular cAMP levels in quiescent and paced cardiomyocytes. Electrical stimulation (1 Hz) caused increased cAMP levels in AdvGFP-infected cardiomyocytes from 336 ± 56 to 473 ± 76 fmol/5 × 10^5 cells, whereas in S100A1-overexpressing cardiomyocytes (AdvS100A1), basal cAMP levels of 374 ± 45 fmol/5 × 10^5 cells raised to 491 ± 51 fmol/5 × 10^5 cells under field stimulation. Statistical analysis revealed no significant influence of S100A1 on cellular cAMP amount in either group. In addition, the PLB phosphorylation state in AdvS100A1-transfected cardiomyocytes showed no significant difference in protein kinase A-

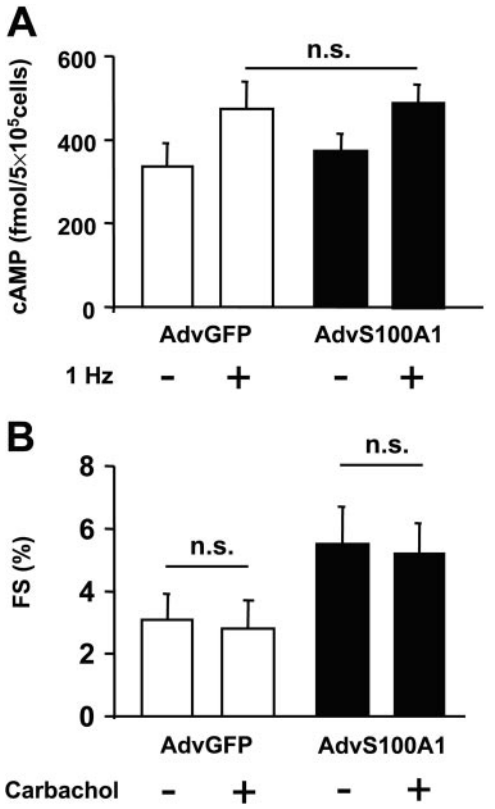

Fig. 5. Effect of S100A1 overexpression on cellular cAMP levels (*A*) and carbachol response (*B*) in control (AvGFP) and S100A1 virus (AdvS100A1) transfected adult rabbit ventricular cardiomyocytes (5×10^5 cells per group). Note that no significant difference between groups was observed. Data are mean ± SEM. *, $P < 0.05$ vs. control ($n = 4$).

dependent phosphorylation at Ser-16, which is downstream to cAMP signaling (PLB-Ser^{16}; Fig. 1*E*). Interestingly, Western blot analysis also failed to document a significant change in the PLB Thr-17 phosphorylation state, indicating that also calmodulin-dependent kinase II activity was not affected by S100A1 (PLB-Thr^{17}; Fig. 1*E*). Importantly, we also found that the S100A1-mediated increase in fractional shortening was not blunted by the administration of carbachol, supporting a cAMP-independent mechanism (Fig. 5*B*).

Discussion

In the early 1980s, Kato and coworkers described the preferential expression of the Ca^{2+} binding protein S100A1 in myocardial tissue (3). Because S100A1 colocalizes with the SR and contractile proteins (4), we postulated that S100A1 is involved in the regulation of cardiac contractility. We therefore investigated the impact of S100A1 overexpression on contractile performance of cellular preparations of cardiac myocytes after S100A1 adenoviral-mediated gene delivery.

In the current study, we observed that S100A1 overexpression significantly improves the inotropic and lusitropic state of isolated cardiac myocytes. This increase of contractile performance after S100A1 gene transfer seems to be a specific effect of S100A1 protein overexpression, as neither the adenovirus infection nor the expression of the reporter protein GFP affected the contractile state in AdvGFP-infected cardiomyocytes as compared with WT cells. Furthermore, control experiments excluded alterations of intrinsic S100A1 expression that might have occurred with gene transfer in AdvGFP-infected cardiomyocytes.

Because the isolated cardiac myocyte only allows the measurement of contractility during unloaded conditions, we examined isometric force generation in a three-dimensional EHT model of neonatal rat cardiomyocytes. Given that neonatal cardiomyocytes possess a higher sensitivity to $[Ca^{2+}]_e$ than adult cardiomyocytes, we performed our measurements in a range of $[Ca^{2+}]_e$ between 0.4 and 2.4 mM (14). Our experiments revealed that S100A1-overexpressing EHTs responded to $[Ca^{2+}]_e$ increments >0.4 mM, with a significantly higher increase of contractile response than AdvGFP-infected EHTs. Thus, S100A1 also remarkably enhances cardiac contractile performance under isometric conditions.

Analyses of intracellular Ca^{2+} transients indicated that S100A1 mediated increases in cell shortening, and force production is mediated at least in part by increased peak systolic $[Ca^{2+}]$ with a significant decrease in time to peak and time to 50% decay. Because the activity of cardiac SR Ca^{2+} ATPase (SERCA2a) is the rate-determining factor of intracellular Ca^{2+} cycling, S100A1 actions might therefore be related to either altered activity or altered expression of the SERCA/PLB complex. The latter was excluded by Western blot analysis, indicating no change in expression of either protein during S100A1 expression. Moreover, there was neither a significant change in cellular cAMP content nor a change in baseline PLB phosphorylation at Ser-16. We furthermore tested the impact of carbachol administration, which is known to blunt inotropic effects in ventricular myocytes only after prior cAMP stimulation, e.g., by receptor agonists, phosphodiesterase inhibitors, forskolin, or cholera toxin (23). The finding that the S100A1-mediated increase in cell shortening was not blunted by the cholinergic receptor agonist carbachol indicates that S100A1 actions are cAMP independent. However, cAMP is known to be highly compartmentalized in cardiac myocytes (24), so our findings do not strictly exclude any cAMP-dependent effect of S100A1.

The Ca^{2+} calmodulin-dependent kinase II is another important regulator of the SERCA/PLB complex relieving PLB inhibition by phosphorylating PLB at Thr-17. Because a S100A1-mediated activation of calmodulin-dependent kinase II could also explain in part the increase of SERCA2a activity, we investigated the phosphorylation state of PLB Thr-17 in S100A1-overexpressing cardiomyocytes. AdvS100A1-infected cardiomyocytes, however, did not show any change in the phosphorylation state of PLB at Thr-17. Therefore, it can be concluded that the S100A1-mediated enhancement of intracellular Ca^{2+} cycling is also calmodulin-dependent kinase II independent.

Because S100A1 colocalizes with the SR (4), it seemed appropriate to choose a model that allows both a direct access for S100A1 to the SR as well as the direct measurement of SR Ca^{2+} uptake to investigate the underlying mechanism of S100A1 Ca^{2+} cycling. For this purpose, we used the model of β-escin skinned cardiomyocytes, which displayed a reproducible Ca^{2+}-dependent stimulation of SERCA2a activity. Given the fact that SERCA2a content in adult rabbit cardiomyocytes was estimated to 7.7 μmol/kg wet weight (25), our calculations revealed a 3:1 molar S100A1/SERCA2a ratio for the addition of 1 μM S100A1. Thus, the observed significant increase of Ca^{2+}-induced SERCA2a activity might be due to a physical interaction of S100A1 with the SERCA2a/PLB complex either by displacing PLB or by altering the Ca^{2+} sensitivity of SERCA2a.

These data confirm that S100A1 modulates the rate-limiting step in intracellular Ca^{2+} cycling by enhancing Ca^{2+}-dependent SR Ca^{2+} uptake rate. Thus, S100A1 may play a pivotal role in diastolic SR Ca^{2+} loading, thereby determining a higher fractional SR Ca^{2+} release and systolic contractile force. Diastolic relaxation is not only determined by SERCA2a activity but is also critically modulated by the Ca^{2+} sensitivity of the cardiac myofilaments (22, 26). Because S100A1 colocalizes with contractile proteins (4), we hypothesized that S100A1 might also

influence myofilament Ca^{2+} sensitivity. In Triton-skinned trabeculae, 1 μM S100A1 protein significantly decreased Ca^{2+} sensitivity and Ca^{2+} cooperativity of the contractile proteins without changing maximal force development. Thus, in addition to troponin C, the most prominent factor that influences Ca^{2+} response of the contractile filaments, S100A1 seems to be another EF-hand Ca^{2+} binding protein affecting myofibrillar Ca^{2+} sensitivity in cardiac muscle. Thus, S100A1 may accelerate diastolic relaxation by enhancing SR Ca^{2+} uptake and decreasing myofilament Ca^{2+} sensitivity, whereas improved systolic function might be related to an enhanced SR Ca^{2+} release due to the increase in SR Ca^{2+} loading.

In light of our findings, it seems reasonable that the significant down-regulation of S100A1 protein levels in end-stage heart failure (6) may contribute to compromised intracellular Ca^{2+} transients and increased myofibrillar Ca^{2+} sensitivity in human cardiomyopathy (7, 27, 28). In contrast, increased S100A1 levels might thus be causally related to an enhanced force production in compensated myocardial hypertrophy (5). Therefore, a therapeutic approach of cardiac S100A1 gene delivery might prove beneficial in the treatment of symptomatic heart failure. Further studies are necessary to identify potential S100A1 target proteins to disclose the molecular mechanisms underlying S100A1-mediated positive physiological effects in cardiac muscle.

We thank Sandy Duncan (Durham), Katrina Wilson (Durham), Aileen Ranken (Glasgow), and Oliver Zeitz (Göttingen) for their excellent technical assistance. This study was supported by the Deutsche Forschungsgemeinschaft (to A.R.; Re 1083/1-1), the British Heart Foundation (to G.S.), and National Institutes of Health R01 Grants HL-59533 and HL-56205 (to W.J.K.).

1. Donato, R. (1999) *Biochim. Biophys. Acta* **1450,** 191–231.
2. Heizmann, C. W. & Cox, J. A. (1998) *Biometals* **11,** 383–397.
3. Kato, K. & Kimura, S. (1985) *Biochim. Biophys. Acta* **842,** 146–150.
4. Haimoto, H. & Kato, K. (1988) *Eur. J. Biochem.* **171,** 409–415.
5. Ehlermann, P., Remppis, A., Guddat, O., Weimann, J., Schnabel, P. A., Motsch, J., Heizmann, C. W. & Katus, H. A. (2000) *Biochim. Biophys. Acta* **1500,** 249–255.
6. Remppis, A., Greten, T., Schafer, B. W., Hunziker, P., Erne, P., Katus, H. A. & Heizmann, C. W. (1996) *Biochim. Biophys. Acta* **1313,** 253–257.
7. Schwartz, A., Sordahl, L. A., Entman, M. L., Allen, J. C., Reddy, Y. S., Goldstein, M. A., Luchi, R. J. & Wyborny, L. E. (1973) *Am. J. Cardiol.* **32,** 407–422.
8. Ehlerman, P., Remppis, A., Most, P., Bernotat, J., Heizmann, C. W. & Katus, H. A. (2000) *J. Chromatogr. B Biomed. Sci. Appl.* **737,** 39–45.
9. He, T. C., Zhou, S., da Costa, L. T., Yu, J., Kinzler, K. W. & Vogelstein, B. (1998) *Proc. Natl. Acad. Sci. USA* **95,** 2509–2514.
10. Schillinger, W., Janssen, P. M., Emami, S., Henderson, S. A., Ross, R. S., Teucher, N., Zeitz, O., Philipson, K. D., Prestle, J. & Hasenfuss, G. (2000) *Circ. Res.* **87,** 581–587.
11. Pollack, P. S., Carson, N. L., Nuss, H. B., Marino, T. A. & Houser, S. R. (1991) *Am. J. Physiol.* **260,** H234–H241.
12. Schagger, H. & von Jagow, G. (1987) *Anal. Biochem.* **166,** 368–379.
13. Drago, G. A. & Colyer, J. (1994) *J. Biol. Chem.* **269,** 25073–25077.
14. Zimmermann, W. H., Fink, C., Kralisch, D., Remmers, U., Weil, J. & Eschenhagen, T. (2000) *Biotechnol. Bioeng.* **68,** 106–114.
15. Bassani, J. W., Bassani, R. A. & Bers, D. M. (1995) *Biophys. J.* **68,** 1453–1460.
16. Smith, G. L., Duncan, A. M., Neary, P., Bruce, L. & Burton, F. L. (2000) *Am. J. Physiol.* **279,** H577–H585.
17. Baudier, J., Glasser, N. & Gerard, D. (1986) *J. Biol. Chem.* **261,** 8192–8203.
18. Janssen, P. M. & de Tombe, P. P. (1997) *Am. J. Physiol.* **273,** H2415–H2422.
19. Janssen, P. M., Zeitz, O., Keweloh, B., Siegel, U., Maier, L. S., Barckhausen, P., Pieske, B., Prestle, J., Lehnart, S. E. & Hasenfuss, G. (2000) *Cardiovasc. Res.* **47,** 99–107.
20. Akhter, S. A., Skaer, C. A., Kypson, A. P., McDonald, P. H., Peppel, K. C., Glower, D. D., Lefkowitz, R. J. & Koch, W. J. (1997) *Proc. Natl. Acad. Sci. USA* **94,** 12100–12115.
21. Eschenhagen, T., Fink, C., Remmers, U., Scholz, H., Wattchow, J., Weil, J., Zimmermann, W., Dohmen, H. H., Schafer, H., Bishopric, N., *et al*. (1997) *FASEB J.* **11,** 683–694.
22. Li, L., Desantiago, J., Chu, G., Kranias, E. G. & Bers, D. M. (2000) *Am. J. Physiol.* **278,** H769–H779.
23. Loffelholz, K. & Pappano, A. J. (1985) *Pharmacol. Rev.* **37,** 1–24.
24. Jurevicius, J. & Fischmeister, R. (1996) *J. Physiol.* **491,** 669–675.
25. Hove-Madsen, L. & Bers, D. M. (1993) *Circ. Res.* **73,** 820–828.
26. Hajjar, R. J., Schwinger, R. H., Schmidt, U., Kim, C. S., Lebeche, D., Doye, A. A. & Gwathmey, J. K. (2000) *Circulation* **11,** 1679–1685.
27. Gwathmey, J. K., Copelas, L., MacKinnon, R., Schoen, F. J., Feldman, M. D., Grossman, W. & Morgan, J. P. (1987) *Circ. Res.* **61,** 70–76.
28. Wolff, M. R., Buck, S. H., Stoker, S. W., Greaser, M. L. & Mentzer, R. M. (1996) *J. Clin. Invest.* **98,** 167–176.